Available online at www.sciencedirect.com

ScienceDirect

IFAC Papers Online CONFERENCE PAPER ARCHIVE

IFAC-PapersOnLine 48-19 (2015) 226–231

Trajectory Tracking of a Quadcopter UAV with Optimal Translational Control ⋆

E.G. Hernandez-Martinez * **G. Fernandez-Anaya** ** **E.D. Ferreira** *** **J.J. Flores-Godoy** **** **A. Lopez-Gonzalez** *

* *Departamento de Ingenierías, Universidad Iberoamericana, Ciudad de México, 01219 México (e-mail: eduardo.gamaliel@ibero.mx)*
** *Departamento de Física y Matemáticas, Universidad Iberoamericana, Ciudad de México, 01219 México, (e-mail: guillermo.fernandez@ibero.mx)*
*** *Departamento de Ingeniería Eléctrica, Universidad Católica del Uruguay, Montevideo, 11600 Uruguay (e-mail: enferrei@ucu.edu.uy)*
**** *Departamento de Matemática, Universidad Católica del Uruguay, Montevideo, 11600 Uruguay (e-mail: jose.flores@ucu.edu.uy)*

Abstract: This paper presents a two-level control strategy for the trajectory tracking of the quadcopter. The external loop is designed to move the translational dynamics of the robot to follow smooth parametric functions using an appropriate variables substitution. The outer loop generates the desired trajectories of the orientation angles, which are controlled in the inner loop. The parameter gains are calculated using linear optimal control in order to minimize the energy consumption of the rotors. The control architecture is designed to be compatible with standard electronic platforms of commercial quadcopters and incorporates the purpose of maximizing flight time, an important requirement in real applications of multi-rotor aerial vehicles. Some numerical simulations show the performance of the control approach.

Keywords: Quadcopter, Optimal Control, Mobile Robots, Trajectory Tracking.

1. INTRODUCTION

Recently, the multi-rotor aerial vehicles have found a wide field of applications in the areas of police and military surveillance, open field exploration, searching and rescue, aerial filming, packages delivering, etc. The related research areas involves aeronautics, mechatronics, dynamical systems, automatic control, signal processing, wireless communication, etc. The hobbyists market and the academical interest has promoted the costs reduction of sensor, actuators and the development of electronic embedded devices dedicated to these aerial vehicles (Lim, 2012). The main interest of the robot control community is to design control strategies to realize autonomous flight following pre-programmed trajectories in the space, converting the multi-rotor platform, driven initially by a radio control, in a fully Unmanned Autonomous Vehicle (UAV).

The quad-rotor setup is the main multi-rotor configuration studied in the control literature due to the simplicity of the modeling and control respect to other platforms and because has the capacity to realize aggressive maneuvers like flip behaviors. It consists on four electrical rotors with propellers mounted at the ends of a cross-shape structure. The dynamical configuration permits the take off and land maneuvers in reduced spaces, hover above targets and the omnidirectional motion in the space. However, the main disadvantage of the quadcopter is the continuous rotation of the actuators which causes a high electrical current spending reducing the practical flight time, commonly in a range of 12 to 18 minutes in commercial platforms (Aranda, 2014). Also, multi-rotor aircrafts are known to be unstable, subject to effects of vibration and noise all the time, and the dynamical control becomes complex if the effects of air turbulence, propellers deflection and other perturbations are incorporated into the dynamical underactuated system model.

In order to simplify the problem, the kinematics and dynamics of a quadcopter can be modeled, discarding environmental perturbations, using the approaches of Newton-Euler, Euler-Lagrange and Quaternions Bertrand (2011). It results in a nonlinear dynamical system with four inputs and six degree of freedom (three cartesian coordinates and three orientation angles). Some works like Gonzalez (2013) deals the case of orientation control for hover flight. In Castillo (2004) is considered take-off landing strategies. As mentioned in Garcia (2013), if the orientation dynamics is faster respect to the translational dynamics, the posture and orientation control laws can be separated in two levels. Example of hierarchical scheme is proposed in Mahony (2012), where the Euler angles in the low level are linearized around zero in order to simplify the trajectory tracking in the high level. Similar focus is presented Aranda (2014) with real-time experiments. The works of Castillo et al (2005) and Escareno (2006) present the linearization of the translational dynamics to track trajectories considering saturated inputs and alternatively,

⋆ The authors acknowledgments the financial support from CONACyT and Universidad Iberomaericana, Mexico City.

10.1016/j.ifacol.2015.12.038

Pyrkin (2014) adds new auxiliar controls dependant of the Euler angles. A similar linearisation technique is given in Minh (2014) which choose a different rotation matrix and does not include the dynamics of the yaw angle. Other works includes the motion coordination of quadcopters teams like Sumano (2013), where the orientation control is approximated in the yaw angle and a consensus error terms are added to the control laws, or the approach of Mahmood (2015), where a change of coordinates is selected to apply a state feedback linearisation. Finally, a wide research about the common PID algorithms programmed in some available embedded controls for multi-rotors is presented in Lim (2012).

Inspired in Escareno (2006), the main contribution of this paper is to propose a separated orientation and posture control to design two input-output linearization control laws, avoiding the approximation of the orientational and translational dynamics, different to the previous works. The control laws clarify the programming of the two control levels in order to be compatible with the standard architecture of commercial embedded controls. Also, the energy saving is addressed using a linear optimal control strategy in in order to maximize the flight time of the quadcopter. Similar works as Ritz (2011); Argentim (2013) add optimal values in the gain parameters of classical controllers, but applied to a reduced linearized quadrotor model only. The performance of the control approach is shown in numerical simulations.

2. KINEMATIC AND DYNAMIC MODEL OF THE QUADCOPTER UAV

A quadcopter vehicle can be conceived as a rigid body with mass and inertia subjected to a gravitational force moving in a $3D$ space. The movement of the vehicle is generated by the combination of the angular velocities of four electrical motors with propellers. They produce one main thrust force applied in the mass center and three moments simultaneously.

According to the figure 1, the position of the body frame Γ_b respect to fixed frame Γ_e is given by $\xi = [x, y, z]^T$.The rotational coordinates of Γ_b respect to Γ_e are defined as $\eta = [\phi, \theta, \psi]^T$. These angles are commonly known as Euler angles (roll, pitch and yaw, respectively). The linear and angular velocities in Γ_b are given by $V = [u, v, w]^T$ and $\Omega = [p, q, r]^T$, respectively. The kinematics of the rigid body describes the relationship of Γ_e respect to Γ_b between the translational and rotational forces. Thus, the translational velocities are given by

$$\dot{\xi} = R_b^e V \tag{1}$$

where R_b^e is the result of the multiplication of the three standard rotations matrices, given by

$$R_x = \begin{bmatrix} 1 & 0 & 0 \\ 0 & \cos\phi & -\sin\phi \\ 0 & \sin\phi & -\cos\phi \end{bmatrix}, R_y = \begin{bmatrix} \cos\theta & 0 & \sin\theta \\ 0 & 1 & 0 \\ -\sin\theta & 0 & \cos\theta \end{bmatrix}$$

$$R_z = \begin{bmatrix} \cos\psi & -\sin\psi & 0 \\ \sin\psi & \cos\psi & 0 \\ 0 & 0 & 1 \end{bmatrix}.$$

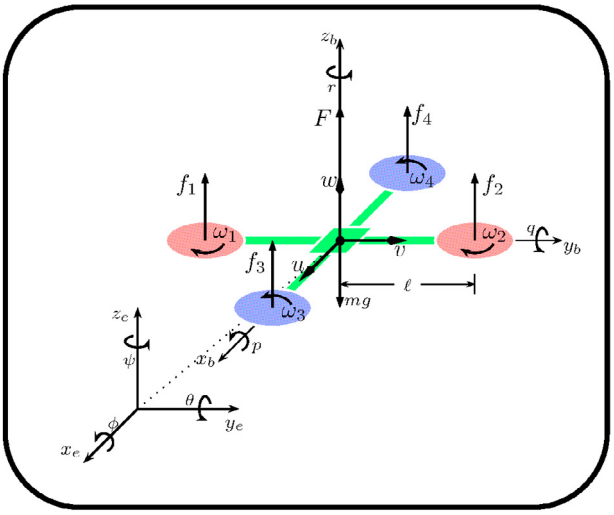

Fig. 1. Quadcopter configuration scheme

It is known that the matrices R_x, R_y and R_z do not commute and different order of multiplication describes a certain sequence of Euler angles. For example, in Aranda (2014), matrix $R_b^e = R_z R_y R_x$, and Escareno (2006) imposes $R_b^e = R_x R_y R_z$. It is clear that the control laws change depending on the selected order of rotations. For major simplicity, in this paper the rotation order selected is $R_b^e = R_z R_y R_x$ given by

$$R_b^e = \begin{bmatrix} c\psi c\theta & -c\theta s\psi & s\theta \\ c\phi s\psi + c\psi s\phi s\theta & c\phi c\psi - s\phi s\psi s\theta & -c\theta s\phi \\ s\phi s\psi - c\phi c\psi s\theta & c\psi s\phi + c\phi s\psi s\theta & c\phi c\theta \end{bmatrix} \tag{2}$$

where $c\phi = \cos\phi$, $c\theta = \cos\theta$, $c\psi = \cos\psi$ and $s\phi = \sin\phi$, $s\theta = \sin\theta$, $s\psi = \sin\psi$. In the other hand, the angular velocity vector η respect to Γ_b using is given by

$$\dot{\eta} = W_n^{-1}\Omega \tag{3}$$

where

$$W_n = \begin{bmatrix} 1 & 0 & -\sin\theta \\ 0 & \cos\phi & \cos\theta\sin\phi \\ 0 & -\sin\phi & \cos\theta\cos\phi \end{bmatrix} \tag{4}$$

The dynamical modeling of the quadcopter represents the evolution of the system due to the forces and torques. Using the focus of Euler-Lagrange and based in Garcia (2013), the dynamical model of the quadcopter is given by

$$m\ddot{\xi} = R_b^e \begin{bmatrix} 0 \\ 0 \\ F \end{bmatrix} + \begin{bmatrix} 0 \\ 0 \\ -mg \end{bmatrix} \tag{5}$$

$$\tilde{J}\ddot{\eta} = \tau - C(\eta, \dot{\eta})\dot{\eta} \tag{6}$$

where m is the mass of the vehicle, F is the main thrust force applied in the center of mass, $\tilde{J} = JW_n$ with J the inertial symmetrical matrix, g is the gravitational constant, $C(\eta, \dot{\eta}) = J\dot{W}_n$ is the Coriolis term and $\tau = [\tau_\phi, \tau_\theta, \tau_\psi]^T$ are the torques generated by the rotors in Γ_b. According to Aranda (2014), the dynamics of the orientation angles can be rewritten using the change of variable.

$$\tau = \tilde{J}\tilde{\tau} + C(\eta, \dot{\eta})\dot{\eta} \tag{7}$$

where $\tilde{\tau} = [\tilde{\tau}_\phi, \tilde{\tau}_\theta, \tilde{\tau}_\psi]^T$ constitutes the vector of auxiliar torques. Thus, substituting the rotational matrix R_b^e given (2) and the torques (7), the dynamical system (5) can be reduced to

$$m\ddot{\xi} = \begin{bmatrix} F\sin\theta \\ -F\cos\theta\sin\phi \\ F\cos\theta\cos\phi - mg \end{bmatrix} \tag{8}$$

$$\ddot{\eta} = \tilde{\tau} \tag{9}$$

Observe that the selection of R_b^e implies that the yaw angle ψ does not appear in the translational dynamics. This property will be exploited in the control strategy in the next section.

As expected, the main thrust force $F = f_1 + f_2 + f_3 + f_4$ where f_i, $i = 1, .., n$ are the individual thrust forces generated by the i-th motor as shown in Figure 1. In this paper we consider all rotors and propellers are similar. Note that the rotors 1 and 2 rotate clockwise producing changes in the angle ϕ and an eventual displacement in the Y axis. Let ℓ be the length of every arm of the quadcopter, then $\tau_\phi = \ell(f_2 - f_1)$. Similarly, the rotors 3 and 4 rotate counterclockwise moving the angle θ and the motion in the X axis. Thus, $\tau_\theta = \ell(f_4 - f_3)$. The torque in the yaw angle is produced by the differences of the rotor pairs $1-2$ and $3-4$, and it is given by $\tau_\psi = \frac{b}{k}[-f_1 - f_2 + f_3 + f_4]$, where k is the thrust constant of every individual array rotor-propeller, and b is the so-called drag constant of the rigid body (Mahony, 2012). Summarizing, the relation of individual thrust forces and the system inputs of (8)-(9) can be written in matrix form as

$$\begin{bmatrix} F \\ \tau \end{bmatrix} = \begin{bmatrix} 1 & 1 & 1 & 1 \\ -\ell & \ell & 0 & 0 \\ 1 & 0 & -\ell & \ell \\ -\frac{b}{k} & -\frac{b}{k} & \frac{b}{k} & \frac{b}{k} \end{bmatrix} \begin{bmatrix} f_1 \\ f_2 \\ f_3 \\ f_4 \end{bmatrix} \tag{10}$$

In a more extended model, the individual forces f_i depend on the angular velocity of the rotor and the features of the propeller (length, pitch angle and deflection), the air turbulence and other environment disturbances. These aerodynamical considerations construct in general a nonlinear actuator dynamics. According to Escareno (2006) and discarding transient effects and disturbances, the forces f_i can be modeled as

$$f_i = k\omega_i^2, i = 1, ..., 4 \tag{11}$$

where ω_i is the angular velocity of the rotor i, and k is the thrust constant mentioned before. This static relation is not very restrictive since the dynamics of the actuators is fast with respect to the motion of the vehicle. In the case of electrical three-phase rotors, commonly used in commercial quadcopters, the internal velocity loop and the power circuit is solved by the so-called Electronical Speed Control (ESC), and the manufacturers provide rotor's datasheets where the force (and indirectly the constant k) is calculated by experimental setups using different propellers. It is clear that a low value of angular velocity requires a less current consumption.

3. CONTROL STRATEGY

As mentioned before, the quadcopter control can be decomposed in two hierarchical levels (posture control and orientation control) assuming that the rotational dynamics converges faster than the translational dynamics. Thus, the control scheme is depicted in Figure 2. The outer loop is related to the posture control designed to follow a desired trajectory in the space. This external controller generates the desired values of the orientation angles for the inner loop. Then, the orientation control moves the angles to desired values using an Inertial Measurement Unit (IMU) sensor, generating a translational motion of the vehicle. It can be measured using some positioning sensors, like GPS for outdoors or videocameras for indoors, closing the loop for the posture control. The inner control also calculates the desired individual forces and angular velocities, which are implemented for the ESC to the rotors.

The control strategy also is designed to be compatible with the commercial control electronics for the quadcopters. As mentioned in Lim (2012), different dedicated microprocessors, like Arducopter, Mikrocopter, Naze32, etc., are designed to implement the orientation control from a remote control communicated by radiofrequency. The radio control sends the desired values of ϕ, θ for a displacement in the axis XY, the value of F to increase o decrease the power to all rotors and modifies indirectly the motion over Z axis, and the desired value of the yaw angle ψ. Note that these four inputs for the inner loop are provided by the outer control, as shown in the Figure 2. It enables the possibility to switch an automatic posture control and a manual control of the angles via remote control in the same experimental platform using some commercial setups.

The next subsection describes the proposed posture and orientation control. The main contributions of the paper appear in the two control levels. For the posture control, we do not use the standard approximation for the translational dynamics, where the control is bounded in a neighborhood around small values of the Euler angles. Also, the control parameters are defined considering the concepts of optimal control, where it is possible to increase the settling time to avoid large values of the control inputs and consequently, a larger energy consumption. In the inner loop, the dynamics of the angles is also linearized and the optimal parameter gains of the posture control are used to design the convergence time of the orientation angles.

3.1 Posture control

In the translational dynamics given in (8), the altitude control is related to the dynamics of the coordinate z, given by

$$m\ddot{z} = F\cos\theta\cos\phi - mg. \tag{12}$$

In order to linearize the dynamics of this coordinate, define the total thrust F as

$$F = \frac{m(r_z + g)}{\cos\theta\cos\phi}. \tag{13}$$

Note that substituting (13) in (12), the dynamics of z now is reduced to $\ddot{z} = r_z$, where r_z is an auxiliar control defined below. The motion in the coordinate Y, is governed, according to (8), by the equation

$$m\ddot{y} = -F\cos\theta\sin\phi. \tag{14}$$

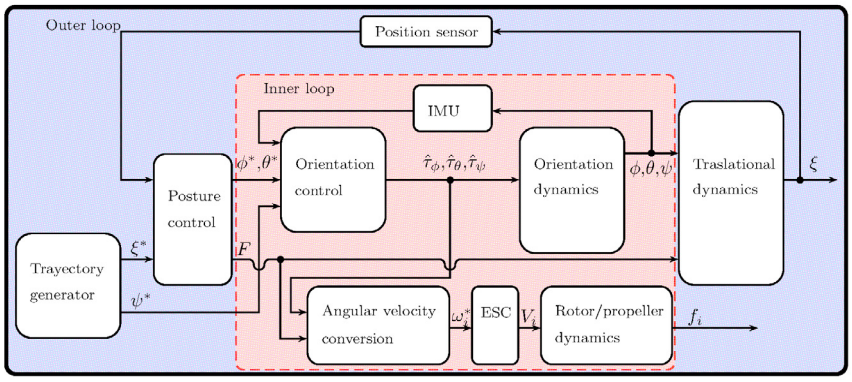

Fig. 2. Control scheme

Substituting the value of F given in (13) in (14), the dynamics of y is reduced to

$$m\ddot{y} = -m(r_z + g)\tan\phi. \tag{15}$$

Similar to the previus case, the dynamics of y can be reduced to

$$\phi = \arctan\left(-\frac{r_y}{r_z + g}\right), \tag{16}$$

and the dynamics of y is reduced to $\ddot{y} = r_y$, where r_y becomes its auxiliar control. Finally, a similar strategy is designed for the motion in the x axis given by

$$m\ddot{x} = F\sin\theta, \tag{17}$$

that can be reduced, substituying (13) in (17), to

$$m\ddot{x} = \frac{m(r_z + g)\tan\theta}{\cos\phi} \tag{18}$$

Note that the x dynamics can be reduced to $\ddot{x} = r_x$ when the value of θ is given by

$$\theta = \arctan\left(\frac{r_x\cos\phi}{r_z + g}\right). \tag{19}$$

In order to obtain an optimal control law in the outer loop, define the position errors as

$$\begin{aligned} e_x &= x - x_d \\ e_y &= y - y_d \\ e_z &= z - zd \end{aligned} \tag{20}$$

where $x_d(t)$, $y_d(t)$ and $z_d(t)$ are the desired twice differenciable trajectories for the coordinates x, y and z, respectively. Recalling the reduced translational dynamics using (13), (16) and (19), the accelerations of these errors are given by

$$\begin{aligned} \ddot{e}_x &= r_x - \ddot{x}_d \\ \ddot{e}_y &= r_y - \ddot{y}_d \\ \ddot{e}_z &= r_z - \ddot{z}_d \end{aligned} \tag{21}$$

Defining new auxiliary inputs $\hat{r}_x = r_x - \ddot{x}_d$, $\hat{r}_y = r_y - \ddot{y}_d$ and $\hat{r}_z = r_z - \ddot{z}_d$, the dynamics of the errors in matrix form are given by

$$\dot{e} = Ae + B\hat{r} \tag{22}$$

where $e = [e_x, \dot{e}_x, e_y, \dot{e}_y, e_z, \dot{e}_z]^T$, $\hat{r} = [\hat{r}_x, \hat{r}_y, \hat{r}_z]^T$,

$$A = \begin{bmatrix} 0&1&0&0&0&0 \\ 0&0&0&0&0&0 \\ 0&0&0&1&0&0 \\ 0&0&0&0&0&0 \\ 0&0&0&0&0&1 \\ 0&0&0&0&0&0 \end{bmatrix}, B = \begin{bmatrix} 0&0&0 \\ 1&0&0 \\ 0&0&0 \\ 0&1&0 \\ 0&0&0 \\ 0&0&1 \end{bmatrix}$$

Then, a static state feedback $\hat{r} = -Ke$ can be defined, where the matrix K is calculated to minimize the cost function

$$J = \int_0^\infty \left(e^T Q e + \hat{r}^T R \hat{r}\right) dt, \tag{23}$$

where $Q = I_{6\times 6}$ and

$$R = \begin{bmatrix} \mu_x & 0 & 0 \\ 0 & \mu_y & 0 \\ 0 & 0 & \mu_z \end{bmatrix}, \tag{24}$$

where the parameters $\mu_x, \mu_y, \mu_z > 1$ can be adjusted to highlight the effect of the input values respect to the time convergence of the position errors. Using the standard optimal approach of Linear Quadratic Regulator (LQR) given in Argentim (2013), the matrix $K = R^{-1}\tilde{B}^T P$, where P is the solution of the Ricatti equation $A^T P + PA - P\tilde{B}R^{-1}\tilde{B}^T P + Q = 0$. The gain matrix K has the form

$$K = \begin{bmatrix} k_{1x} & k_{2x} & 0 & 0 & 0 & 0 \\ 0 & 0 & k_{1y} & k_{2y} & 0 & 0 \\ 0 & 0 & 0 & 0 & k_{1z} & k_{2z} \end{bmatrix}, \tag{25}$$

therefore, the control inputs result in

$$\begin{aligned} r_x &= \ddot{x}_d + \hat{r}_x = \ddot{x}_d - k_{2x}\dot{e}_x - k_{1x}e_x \\ r_y &= \ddot{y}_d + \hat{r}_y = \ddot{y}_d - k_{2y}\dot{e}_y - k_{1y}e_y \\ r_z &= \ddot{z}_d + \hat{r}_z = \ddot{z}_d - k_{2z}\dot{e}_z - k_{1z}e_z \end{aligned} \tag{26}$$

Note that substituting (26) in (21), result three second order linear functions of the errors ensuring their convergence to zero. The settling time and damping coefficient for the three error are given respectively by

$$t_{ssx} = \frac{10}{k_{2x}}, t_{ssy} = \frac{10}{k_{2y}}, t_{ssz} = \frac{10}{k_{2z}}, \tag{27}$$

$$\xi_x = \frac{k_{2x}}{2\sqrt{k_{1x}}}, \xi_y = \frac{k_{2y}}{2\sqrt{k_{1y}}}, \xi_z = \frac{k_{2z}}{2\sqrt{k_{1z}}}. \tag{28}$$

As expected, a great value of μ_x, μ_y and μ_z increases the settling time and the time convergence. However, it generates low values of the control inputs which is translated in less angular velocities of the rotors, saving energy and maximizing the flight time. The parameters μ_x, μ_y and μ_z must be adjusted according to the rate change of the desired trajectories to achieve the gathering between and acceptable convergence time and the energy consumption.

Observe that the posture control generates the desired values of F, ϕ, and θ, which becomes in the desired setpoints for the orientation control (inner loop). In the computational order of these control laws, the value of ϕ (depending of r_y only) is calculated in a first step according to (16). It is substituying in (19) to calculate θ, and finally the values of the two previous angles are substituying in (13) to find the value of F. Note that the posture control requires only the coordinate ξ and the information of the desired trajectories x_d, y_d and z_d. Remember that the yaw angle ψ do not appear in the translational dynamics as mentioned before. It is addressed in the next section.

3.2 Orientation control

Define as $\eta_d = [\phi_d, \theta_d, \psi_d]$ the desired twice differenciable trajectories for the orientation angles η. As show in the figure 2, the desired values of ϕ_d, θ_d are provided by the posture control through (16) and (19). The desired trajectory ψ_d for the yaw angle can be defined by the user because remains independent of the posture control. A possible selection of ψ_d could be define to achieve a yaw angle according to the velocity vector generated by x_d and y_d, i.e. $\psi_d = \arctan \frac{\dot{y}_d}{\dot{x}_d}$, and the vehicle will point to the forward direction of the path in the XY plane.

Define the auxiliary control inputs given in (9) as

$$\begin{aligned}\tilde{\tau}_\phi &= \ddot{\phi}_d - k_{2\phi}(\dot{\phi} - \dot{\phi}_d) - k_{1\phi}(\phi - \phi_d)\\ \tilde{\tau}_\theta &= \ddot{\theta}_d - k_{2\theta}(\dot{\theta} - \dot{\theta}_d) - k_{1\theta}(\theta - \theta_d)\\ \tilde{\tau}_\psi &= \ddot{\psi}_d - k_{2\psi}(\dot{\psi} - \dot{\psi}_d) - k_{1\psi}(\psi - \psi_d)\end{aligned} \tag{29}$$

Note that substituying (29) in (9), it is constructed a linear equation of the angle errors given by $e_\phi = \phi - \phi_d$, $e_\theta = \theta - \theta_d$ and $e_\psi = \psi - \psi_d$. To ensure a fast convergence of the orientation angles without overdamped responses, it is suggested to define

$$k_{2\phi} = k_{2\theta} = k_{2\psi} = \frac{10}{\rho\left(\min\left\{t_{ssx}, t_{ssy}, t_{ssz}\right\}\right)}, \tag{30}$$

$$k_{1\phi} = \sqrt{\frac{k_{2\phi}}{2}}, k_{1\theta} = \sqrt{\frac{k_{2\theta}}{2}}, k_{1\psi} = \sqrt{\frac{k_{2\psi}}{2}}, \tag{31}$$

where $0 < \rho < 1$ to establish a less settling time respect than the translational convergence. Finally, using the values of F obtained in (13) and the three main torques of (29), the angular velocities of the rotors send to the ESC's, using the equation (10) and substituying the values of (11), become in

$$\begin{bmatrix}\omega_1^2\\ \omega_2^2\\ \omega_3^2\\ \omega_4^2\end{bmatrix} = \frac{1}{k}\begin{bmatrix}1 & 1 & 1 & 1\\ -\ell & \ell & 0 & 0\\ 1 & 0 & -\ell & \ell\\ -\frac{b}{k} & -\frac{b}{k} & \frac{b}{k} & \frac{b}{k}\end{bmatrix}^{-1}\begin{bmatrix}F\\ \tau\end{bmatrix} \tag{32}$$

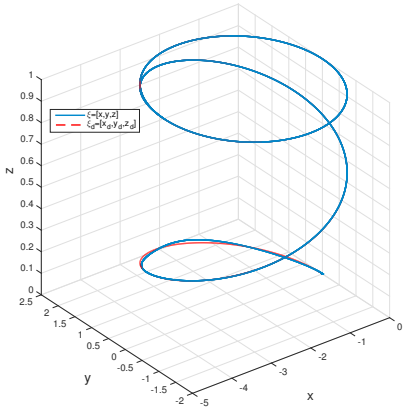

Fig. 3. Trajectory of the quadcopter in the space

where τ is calculated from (7) and (29).

4. NUMERICAL SIMULATION

Figures 3-6 show a numerical simulation of the control approach using Matlab-Simulink©. The desired trajectory is a circular path for the coordinates x and y, i.e. $m_{xd} = -2 + 2\cos(\frac{2\pi}{20}t)$, $m_{yd} = 2\sin(\frac{2\pi}{20}t)$ (in meters), and a smooth polinomial funtion for z, i.e. $m_{zd} = \frac{3}{30^2}t^2 - \frac{2}{30^3}t^3$ for $t < 30$ and $m_{zd} = 1$, for $t \geq 30$. Also, is defined $\psi_d = 0$, $\forall t > 0$. The initial conditions are $\xi(0) = [0, 0, 0]^T$ and $\eta(0) = [0, 0, \frac{pi}{4}]$.

For the posture control, $\mu_x = \mu_y = \mu_z = 2$, producing the optimal gains $k_{1x} = k_{1y} = k_{1z} = 0.7071$ and $k_{2x} = k_{2y} = k_{2z} = 1.3836$. Thus, the settling time and damping are fixed respectively by $t_{ssx} = t_{ssy} = t_{ssz} = 7.2278$ and $\xi_x = \xi_y = \xi_z = 0.8227$. Then, for the orientation control, the parameter gains are selected with $\rho = 0.2$ as $k_{2\phi} = k_{2\theta} = k_{2\psi} = \frac{10}{\rho(7.2278)} = 6.9177$ and $k_{1\phi} = k_{1\theta} = k_{1\psi} = \sqrt{\frac{6.9177}{2}} = 1.8597$.

As shown in the figure 3 and figure 4 the quadcopter achieves the desired trajectory and the orientation angles follow the desired values imposed by the posture control. Also, the convergence to the desired values is shown in the figure 5 where the errors converge to zero. Finally, the figure 6 shows the control inputs generated by the two control levels.

5. CONCLUSION

This paper presents a hierarchical two-level control scheme for the trajectory tracking of the quadcopter UAV. In the posture control, a change of variables is designed to generate the desired values of the angles and the main thrust force for the orientation control. The control laws do not use some approximation of the original nonlinear dynamics of the vehicle. The parameter gains are selected according to the LQR method in order to increase the settling time and reduce the magnitude of inputs in order to save energy. On the other hand, the orientation control defines its gain parameters according to the optimal gains of the outer loop. It ensures that the orientation dynamics

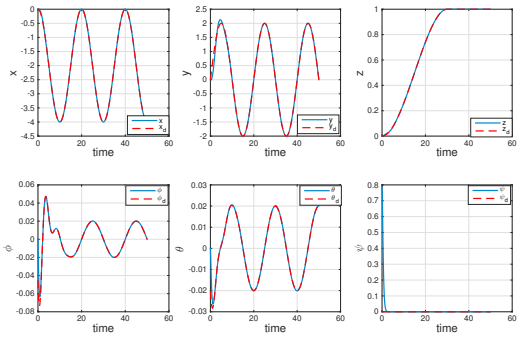

Fig. 4. Graphics of ξ and η

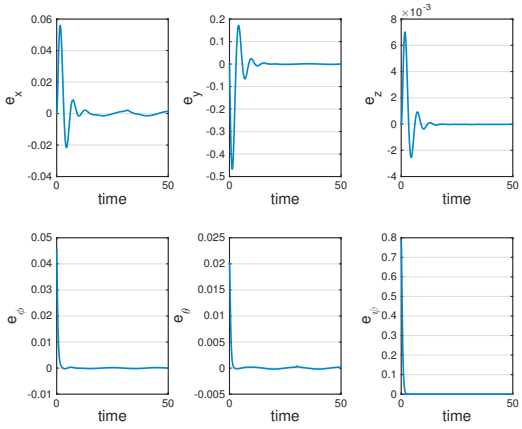

Fig. 5. Graphics of posture and orientation errors

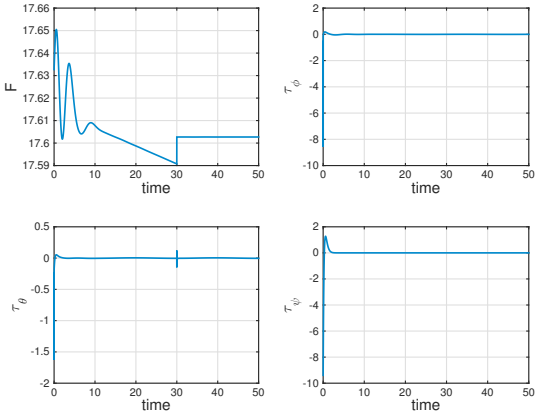

Fig. 6. Graphics of control inputs

is faster than the translational dynamics. The performance of the control scheme is shown in a numerical simulation. The design of the control laws can be compatible with the commercial platforms for the contruction of UAV's. As further research, the control scheme will be tested in a real quadcopter.

ACKNOWLEDGEMENTS

The author aknowledges the finantial support from CONACyT by the project grant 216763, and the Universidad Iberoamericana, Mexico City.

REFERENCES

H. Lim, J, Park, D. Lee and H.J. Kim Build your own quadrotor. *IEEE Robot. Autom. Mag.*, volume 19, no. 3, pp 33–45, 2012.

J. Santiaguillo-Salinas and E. Aranda-Bricaire Trajectory following for a A.R. Drone four-rotor helicopter using ROS (in spanish). *In the Proc. of XVI Congreso Latinoamericano de Control Automático CLCA*, pages 606–611, 2014.

S. Bertrand, N. Guenard, T. Hamel, H. Piet-Lahanier and L. Eck A hierarchical controller for miniature VTOL UAV's: Design and stability analysis using singular perturbations theory. *ELSEVIER Control Engineering Practice*, volume 19, no. 1, pages 1099–1108, 2011.

I. Gonzalez, S. Salazar, J. Torres, R. Lozano and H. Romero Real-Time attitude stabilization of a mini-UAV quad-rotor uring speed feedback. *Journal of Intelligent Robotic Systems*, volume 70, no. 4, pages 93–106, 2013.

P. Castillo, R. Lozano and A. Dzul Stabilization of a mini-rotorcraft having four rotors. *In Proc. of the 2004 IEEE/RSJ International Conference on Intelligent Robots and Systems (IROS)*, pages 2693-2698, 2004.

L.R. Garcia, A.E. Dzul, R. Lozano and C. Pergard. Quad rotocraft control. Vision-Based Hovering and Navigation. In R. Lozano, editor, *Advances in Industrial Control*, volume 1, pages 23–34. Springer, 1st edition, 2013.

R. Mahony, V. Kumar and P. Corke Multirotor aerial vehicles: modeling, estimation, and control of quadrotor. *IEEE Robot. Autom. Mag.*, volume 19, no. 3, pages 20–32, 2012.

P. Castillo Garcia, R. Lozano and A.R. Dzul Modelling and Control of Mini-Flying Machines. In R. Lozano, editor, *Advances in Industrial Control*, volume 1, pages 39–52. Springer, 1st edition, 2005.

J. Escareno, S. Salazar-Cruz and R. Lozano Embedded control of a four-rotor UAV. *Proc. of the American Control Conference*, pp 3936–3941, 2006.

A.A. Pyrkin, A.A. Bobtsov, S.A. Kolyubin, O.I. Borisov and V.S. Gromov Output controller for quadcopters based on mathematical model decomposition *In Proc. of the 22nd Mediterranean Conference of Control and Automation (MED)*, pages 1281-1286, 2014.

Q.H. Minh, Z. Weihua and X. Lihua L1 adaptive control for quadcopter: Design and implementation *In Proc. of the 13th Int. Conf. on Control Automation Robotics and Vision (ICARCV)*, pages 1496-1501, 2014.

E. Sumano, R. Castro and R. Lozano Sinchronization of quadrotos in coordinated manner (in spanish). *Congreso Nacional de Control Automático*, 2013.

A. Mahmood and K. Yoonsoon Decentralized formation control of quadcopters using feedback linearization *In Proc. of the 6th Int. Conf. on Automation, Robotics and Applications (ICARA)*, pages 537-541, 2015.

R. Ritz, M. Hehn, S. Lupashin, R. D'Anrea Quadrocopter performance benchmarking using optimal control *In Proc. of the 2011 IEEE/RSJ International Conference on Intelligent Robots and Systems (IROS)*, pages 5179-5186, 2011.

L.M. Argentim, W.C. Rezende, P.E. Santos and R.A. Aguiar PID, LQR and LQR-PID on a quadcopter platform *In Proc. of the International Conference on Informatics, Electronics and Vision (ICIEV)*, pages 1-6, 2013.